Anisotropies of in-phase, out-of-phase, and frequency-dependent susceptibilities in three loess/palaeosol profiles in the Czech Republic; methodological implications

FRANTIŠEK HROUDA[1,2], MARTIN CHADIMA[1,3], JOSEF JEŽEK[2] AND JAROSLAV KADLEC[4]

1 AGICO Ltd., Ječná 29a, 621 00 Brno, Czech Republic, e-mail: fhrouda@agico.cz

2 Faculty of Science, Charles University, Albertov 6, 128 43 Praha 2, Czech Republic

3 Institute of Geology CAS, Rozvojová 269, 165 00 Praha 6, Czech Republic

4 Institute of Geophysics CAS, Boční II/1401, 141 31 Praha 4, Czech Republic

Received: January 2, 2017; Revised: May 9, 2017; Accepted: July 14, 2017

ABSTRACT

The relationship between the anisotropy of frequency-dependent magnetic susceptibility (fdAMS) and the anisotropy of out-of-phase magnetic susceptibility (opAMS) was investigated theoretically and also empirically at three loess/palaoesol profiles in Prague and in Southern Moravia. The data treatment was made in terms of mean susceptibility, degree of AMS, and orientations of principal susceptibilities. It has shown that the fdAMS and opAMS can serve as indicators of the preferred orientations of ultrafine magnetic particles that are on transition between superparamagnetic and stable single domain states in rocks, soils and environmental materials. In loess/palaeosol sequences, the fdAMS and opAMS correlate reasonably, because they are due to magnetic particles of similar grain sizes. The fdAMS and opAMS can be both coaxial with standard AMS (i.e. anisotropy of in-phase susceptibility - ipAMS) or non-coaxial indicating slightly different orientations of viscous magnetic particles.

Keywords: anisotropy, out-of-phase susceptibility, frequency-dependent susceptibility, loess/palaeosol sequence, ultrafine particles, magnetic fabric

1. INTRODUCTION

In the eolian sediments, such as loess, the anisotropy of magnetic susceptibility (AMS) is widely used in the determination of the palaeo-wind directions and in the investigation of the mechanisms of the dust deposition and loess lithification as well as in the identification of post-depositional and post-diagenetic processes (e.g., *Liu et al., 1988, 2008*; *Lagroix and Banerjee, 2002, 2004a,b*; *Hus, 2003*; *Matasova and Kazansky, 2004*; *Zhu et al., 2000*; *Bradák, 2009*; *Bradák et al., 2011*; *Bradák and Kovácz, 2014*; *Antoine et al., 2014*; *Taylor and Lagroix, 2015*).

 Stud. Geophys. Geod., 62 (2018), 272–290, DOI: 10.1007/s11200-017-0701-y

The magnetic minerals carrying the AMS in loess/palaeosol sequences are represented by both paramagnetic (e.g. clay minerals) and ferromagnetic minerals such as magnetite and/or maghemite. The last are characterized by wide span in grain size ranging from ultrafine superparamagnetic (SP), through single domain (SD) to multi domain (MD) particles. The presence of magnetically viscous SP particles can be most comfortably indicated or even assessed semi-quantitatively by the investigation of frequency-dependent susceptibility (for summary see for instance *Heller and Evans, 2003*; *Hrouda, 2011*) or newly also by the out-of-phase susceptibility (*Hrouda et al., 2013*). The theoretical relationship between these susceptibilities is described by the $\pi/2$ law valid for materials the latter susceptibility of which is solely due to the viscous phenomena and not due to electrical eddy currents or weak field hysteresis, which is valid for both magnetite and maghemite (e.g., *Néel, 1949*; *Jackson, 2003*). The correlation between the frequency-dependent susceptibility and the out-of-phase susceptibility in loess/palaeosol sequences is excellent and even semi-quantitative conversion between these two susceptibilities is possible (*Hrouda et al., 2013*). As the out-of-phase susceptibility is measured simultaneously with the in-phase susceptibility during one measuring process with some instruments and provides us with more or less the same information as does the frequency-dependent susceptibility, it is recommended to be routinely investigated in solving various problems of environmental magnetism. This is very useful for economic reasons in working with large specimen collections as in palaeoclimatology and environmental magnetism.

The preferred orientation of magnetically viscous SP particles can be investigated through the anisotropy of frequency-dependent susceptibility (fdAMS) and, newly, also through the anisotropy of out-of-phase susceptibility (opAMS) (*Hrouda and Ježek, 2014*; *Hrouda et al., 2017*). The advantage of the opAMS compared to fdAMS lies in its simultaneous measurement with the anisotropy of in-phase susceptibility (ipAMS), while the fdAMS requires separate measurements at least at two operating frequencies. For this reason, the opAMS has theoretical potential to substitute the fdAMS in environmental magnetism studies (*Hrouda et al., 2013*). Unfortunately, very little is known of the relationship between the fdAMS and opAMS. In the following, the prefixes ip, op and fd stand for in-phase, out-of-phase and frequency-dependent, respectively.

The purpose of the present paper is fill this gap through theoretical investigations of the opAMS and fdAMS of magnetically viscous particles and through experimental investigation of opAMS and fdAMS on specimens of three loess/palaeosol sections in the Czech Republic. The research is oriented methodologically and has only limited ambitions to get geological information. For this reason and because the contents of magnetically viscous particles may sometimes change continuously regardless of lithology, the loess and soil layers are not treated separately.

2. THEORY

A characteristic feature of the dynamic susceptibility of the magnetically viscous particles, i.e. those that are on the transition between SP and SSD state, is that it resolves into a component that is in-phase with applied field and a component that is out-of-phase (e.g., *Néel, 1949*; *Jackson, 2003*; *Shcherbakov and Fabian, 2005*; *Egli, 2009*). On the other hand, the susceptibility of diamagnetic, paramagnetic and many ferromagnetic materials is entirely in-phase, with the out-of-phase susceptibility being effectively zero.

2.1. Susceptibility of magnetically viscous particles

The susceptibility of these particles can be described by the formula introduced by *Néel (1949)* and transcribed by *Egli (2009)*, using terms of linear dynamic susceptibility $\kappa = \kappa' - \mathrm{i}\kappa''$, as follows

$$\kappa_{SP/SD} = \kappa_{SD}\left(\frac{\beta}{1+\mathrm{i}\,\tau_0\omega \mathrm{e}^{\beta}}+1\right), \tag{1}$$

where $\kappa_{SD} = 2M_s/3H_k$, $\beta = K_aV/k_BT$ and $\omega = 2\pi f_m$; M_s is saturation magnetization, H_k is microscopic coercivity related to macroscopic coercivity H_c as $H_k = 2.09H_c$ (*Worm, 1998*), K_a is the anisotropy constant, V is particle volume, k_B is the Boltzmann constant, T is absolute temperature, $\tau_0 \approx 10^{-10}$ s is a time constant, and f_m is operating frequency. The in-phase susceptibility then is (e.g., *Hrouda, 2011*)

$$\kappa' = \kappa_{SD}\left[\frac{\beta}{1+\left(\tau_0\omega \mathrm{e}^{\beta}\right)^2}+1\right]. \tag{2}$$

Figure 1a shows the in-phase susceptibility vs. particle diameter plot for the operating frequencies of the MFK1-FA and KLY5-A Kappabridges for magnetite ($K_a = 2.5 \times 10^4$ J m^{-3}, see *Hrouda, 2011*). Initially, the susceptibility increases almost linearly with grain size and after reaching its maximum value it acutely decreases down to SSD susceptibilities. It is the largest for the lowest operating frequency (976 Hz) and decreases with increasing frequency being the smallest at the highest operating frequency (15616 Hz). Figure 1b shows, among others, the differences between the in-phase

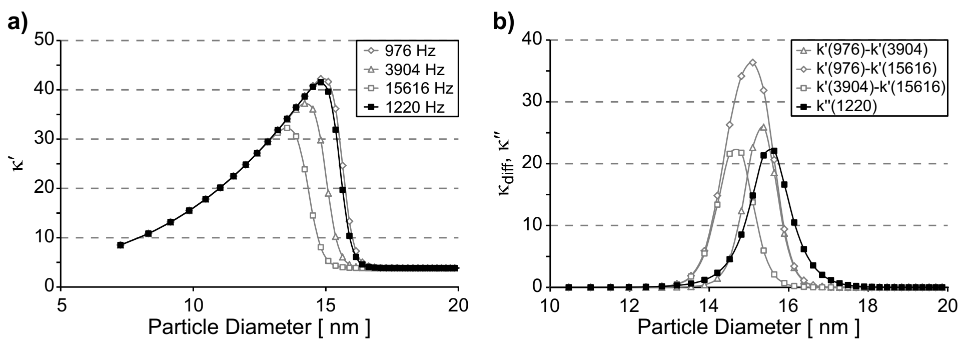

Fig. 1. **a)** In-phase susceptibility κ' at the frequencies of the MFK1 and KLY-5 Kappabridges as function of diameter of spherical particles of magnetite; **b)** differences in the in-phase susceptibilities κ_{diff} at the MFK1 Kappabridge frequencies and the out-of-phase susceptibility κ'' at the KLY-5 Kappabridge frequency for the same particles.

susceptibilities at the frequencies of the MFK1-FA Kappabridge vs. particle diameter. Initially, the differences are effectively zero, then they increase creating bell-like curves and subsequently they drop to effective zero.

The out-of-phase susceptibility of magnetically viscous particles is (e.g., *Hrouda et al., 2013*)

$$\kappa'' = \kappa_{SD} \frac{\beta \tau_0 \omega e^{\beta}}{1 + \left(\tau_0 \omega e^{\beta} \right)^2} . \tag{3}$$

Figure 1b shows, in addition to susceptibility differences, also the out-of-phase susceptibility vs. particle diameter at the frequency of the KLY5-A Kappabridge. Initially, the out-of-phase susceptibility is effectively zero then it increases creating bell-like curve and subsequently dropping to effective zero. It should be noted that the bell-like curves of the in-phase susceptibility differences and the bell-like curve of the out-of-phase susceptibility are near one another indicating that both the phenomena are controlled by the magnetic particles of similar grain sizes. In addition, whereas the in-phase susceptibility is controlled by all minerals in the rock, including the ferromagnetic particles of relatively wide grain-size interval, the frequency-dependent in-phase susceptibility and the out-of-phase susceptibility are dominantly affected by the particles of much narrower interval controlled by the operating frequencies used.

Néel (1949) showed that for population of grains with a wide distribution of relaxation times, the out-of-phase susceptibility is proportional to the frequency-dependence of the in-phase susceptibility (see also *Jackson, 2003*). This relationship is called the $\pi/2$ law and can be written as follows (cf. *Jackson, 2003*; *Egli, 2009*)

$$\kappa'' = -\frac{\pi}{2} \frac{\partial \kappa'}{\partial \ln f_m} . \tag{4}$$

Let us introduce an analogous parameter for the frequency-dependent susceptibility

$$\kappa_{diff} = -\frac{\pi}{2} \frac{\kappa'_{LF} - \kappa'_{HF}}{\ln f_{mLF} - \ln f_{mHF}} , \tag{5}$$

where the indices *LF* and *HF* denote the low and high frequency, respectively. It can be said that this formula represents the finite difference version of the $\pi/2$ law.

2.2. Grain AMS of magnetically viscous particles

In these particles, the static (DC) equilibrium susceptibilities parallel (||) and perpendicular ($\perp$) to the easy magnetization axis are (*Shliomis and Stepanov, 1993*; *Svedlindh et al., 1997*)

$$\kappa_{||} = \mu_0 \frac{M_s^2 V}{k_B T} \frac{R'}{R} , \qquad \kappa_{\perp} = \mu_0 \frac{M_s^2 V}{k_B T} \frac{R - R'}{2R} , \tag{6}$$

where R and R' are integral functions of $\sigma = K_a V / k_B T$ (for details see *Svedlindh et al., 1997*; *Hrouda and Ježek, 2014*).

The dynamic (AC) susceptibility, which can be resolved into in-phase and out-of-phase components, is (*Shliomis and Stepanov, 1993*; *Svendlidh et al., 1997*)

$$\kappa'_{\|} = \frac{\kappa_{\|}}{1+\left(\omega\tau_{\|}\right)^2}, \quad \kappa'_{\perp} = \frac{\kappa_{\perp}}{1+\left(\omega\tau_{\perp}\right)^2}, \tag{7a}$$

$$\kappa''_{\|} = \frac{\kappa_{\|}\omega\tau_{\|}}{1+\left(\omega\tau_{\|}\right)^2}, \quad \kappa''_{\perp} = 0, \tag{7b}$$

where $\tau_{\|} = \tau_0 \exp\left(\sigma\right)$ (τ_0 is in the order of 10^{-10} s) and $\tau_{\perp}$ is of the order of τ_0.

Figure 2a shows variation of the degree of ipAMS (here defined as $P = \kappa'_{\|}/\kappa'_{\perp}$) with particle diameter for magnetite grain. The degree of ipAMS increases with the particle diameter, converging to infinitely values high in SD particles.

2.3. Degrees of ipAMS and opAMS of ensembles of magnetically viscous particles

In magnetically monomineralic rocks, the AMS is controlled by both the grain AMS of the magnetic mineral and the preferred orientation of it (e.g., *Hrouda, 1982*; *Tarling and Hrouda, 1993*). In the AMS models, the preferred orientation may be characterized by the orientation tensor, which, for uniaxial magnetic grains, is defined as follows (*Scheidegger, 1965*; *Ježek & Hrouda, 2000*)

$$\mathbf{E} = \frac{1}{n}\begin{pmatrix} \sum l_i^2 & \sum l_i m_i & \sum l_i n_i \\ \sum m_i l_i & \sum m_i^2 & \sum m_i n_i \\ \sum n_i l_i & \sum m_i n_i & \sum n_i^2 \end{pmatrix}, \tag{8}$$

where l_i, m_i, n_i are the direction cosines of the i-th grain axis and n is the number of the grains considered. The principal values of this tensor ($E_1 \geq E_2 \geq E_3$) have the property $E_1 + E_2 + E_3 = 1$. This tensor is related to the susceptibility tensor as follows (see *Ježek and Hrouda, 2000*)

$$\mathbf{k} = k\mathbf{I} + \Delta\mathbf{E}, \tag{9}$$

where **k** is rock susceptibility tensor, **I** is identity matrix, and k is the apparent mineral susceptibility in general. For prolate spheroids, $k = k_2 = k_3$, $\Delta = k_1 - k$ ($k_1 \geq k_2 \geq k_3$ are the grain principal susceptibilities) and **E** is orientation tensor of the grain maximum susceptibility axes. For oblate spheroids, $k = k_1 = k_2$, $\Delta = k - k_3$ and **E** is orientation tensor of grain minimum susceptibility axes.

The above relationship was used to investigate the effect of the different degrees of grain fdAMS and opAMS. Namely, *Hrouda (1980)* showed that the degree of AMS of the rock whose AMS is carried by very strongly anisotropic grains ($P > 100$) is solely controlled by the preferred orientation of the grains. As the grain degree of fdAMS can be

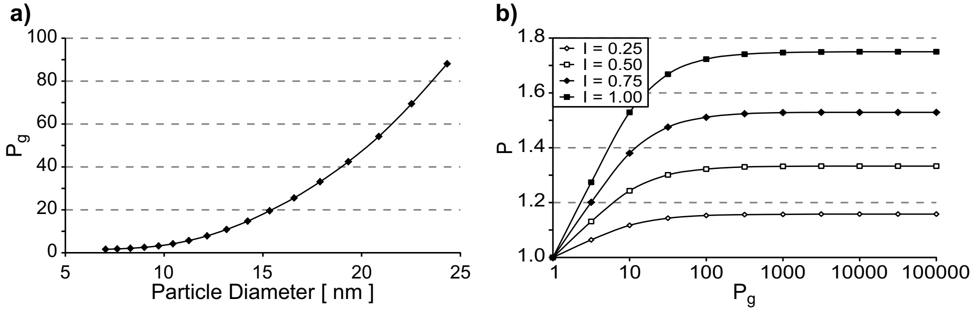

Fig. 2. **a)** Degree of grain AMS (defined as $P_g = \kappa'_{||}/\kappa'_{\perp}$) as a function of particle diameter for magnetite at room temperature at 1 kHz operating frequency, and **b)** variation of degree of ipAMS (P) in dependence of the grain degree of AMS P_g for several values of the I parameter (Eq. (10)), characterizing the intensity of preferred orientation of the grain axes (after *Hrouda and Ježek, 2017*).

very high (see Fig. 2a) and that of opAMS is even infinitely high, a question arises how these differences result in the fdAMS and opAMS of ensembles of weakly oriented particles. Fig. 2b shows the variation of the degree of AMS of the model according to I parameter characterizing the intensity of preferred orientation of the grain axes for several values of the grain degree of AMS. The I parameter is defined as (*Lisle, 1985*)

$$I = \frac{15}{2} \sum_{i=1}^{3} \left(E_i - \frac{1}{3} \right)^2 , \qquad (10)$$

where E_i ($i = 1, 2, 3$) are principal values of the orientation tensor. It can vary from 0 for isotropic fabric to 5 for the fabric in which all grain axes are perfectly parallel to one another. It is obvious from Fig. 2b that the model degree of AMS increases with increasing intensity of the orientation of particle axes and, though much less, with the grain degree of AMS.

3. INSTRUMENTATION, PARAMETERS USED

The ipAMS, fdAMS, and opAMS were measured by the MFK1-FA and KLY5-A Kappabridges. The former Kappabridge measures the AMS at three operating frequencies with the precision sufficient for reliable determination of the fdAMS (*Pokorný et al., 2011*; *Hrouda and Pokorný, 2011, 2012*). The latter Kappabridge, which works at one operating frequency, is equipped to measure simultaneously both the in-phase and out-of-phase susceptibilities and their anisotropies (*Pokorný et al., 2016*). Unlike the MFK1-FA Kappabridge, which measures only the relative changes of the out-of-phase susceptibility, the KLY5-A Kappabridge measures the out-of-phase susceptibility “absolutely’’ (with no shift of the origin). The precision in the determination of the anisotropy of in-phase susceptibility (ipAMS) is at least comparable to or even slightly better than that in the MFK1-FA Kappabridge. The fdAMS was measured at the operating frequencies 976 Hz and 15616 Hz in the field 200 A m^{-1}. The ipAMS and opAMS were measured in the field 400 A m^{-1} peak at the operating frequency 1220 Hz at room temperature and computed by the SAFYR (ver. 6) program. The calculus for computation of the opAMS is exactly the same as that for computation of the ipAMS. Both the anisotropies are determined during one measuring process.

It is usual to represent the susceptibility tensor by convenient parameters derived from principal susceptibilities (e.g., *Nagata, 1961*; *Jelínek, 1981*), for instance

$$K_m = \frac{K_1 + K_2 + K_3}{3}, \quad P = \frac{K_1}{K_3}, \quad T = \frac{2\eta_2 - \eta_1 - \eta_3}{\eta_1 - \eta_3} = 2\frac{\ln F}{\ln P} - 1, \tag{11}$$

where $K_1 \geq K_2 \geq K_3$ are the principal susceptibilities, $\eta_1 = \ln K_1$, $\eta_2 = \ln K_2$, $\eta_3 = \ln K_3$, and $F = K_2/K_3$. The parameter K_m is called the mean susceptibility and characterizes the qualitative and quantitative content of magnetic minerals in a rock. The parameter P, called the degree of AMS, indicates the intensity of the preferred orientation of magnetic minerals in a rock. The parameter T, called the shape parameter, characterizes the symmetry or shape of the AMS ellipsoid. If $0 < T < 1$, the AMS ellipsoid is oblate (the magnetic fabric is planar); $T = +1$ means that the AMS ellipsoid is rotationally symmetric (uniaxial oblate). If $-1 < T < 0$, the AMS ellipsoid is prolate (the magnetic fabric is linear); $T = -1$ means that the AMS ellipsoid is uniaxial prolate.

In order to obtain a statistical evaluation of the AMS tensors, the ANISOFT package of programs (*Jelínek, 1978*; *Chadima and Jelínek, 2008*) can be used, which enable a complete statistical evaluation of a group of specimens to be carried out; the mean principal directions are determined as well as the confidence areas around them on the likelihood level 95%.

The frequency-dependent susceptibility can be characterized by the following commonly accepted parameter introduced by *Dearing et al. (1996)* and called the percentage loss of susceptibility

$$K_{FD} = \frac{K_{LF} - K_{HF}}{K_{LF}}, \tag{12}$$

expressed in %, where K_{LF}, K_{HF} are susceptibilities at the lower and higher frequencies, respectively. In environmental magnetism, this parameter is usually calculated from mass susceptibilities being then denoted χ_{FD}; nevertheless, it holds $K_{FD} = \chi_{FD}$. Sometimes, it is advantageous to work with simple susceptibility difference

$$K_{FV} = K_{LF} - K_{HF}, \tag{13}$$

called by *Dearing et al. (1996)* the relative loss of susceptibility, being given in units of susceptibility.

The out-of-phase susceptibility can be characterized by the phase angle δ

$$\tan\delta = \frac{\kappa''}{\kappa'}, \tag{14}$$

informing us of the delay of the out-of-phase response behind the in-phase response.

4. GEOGRAPHICAL POSITION AND CONCISE GEOLOGICAL SETTING

The ipAMS, fdAMS, and opAMS investigations were performed on sediments collected from three loess/palaeosol sections exposed in southern Moravia (Bulhary section, located 48.8344486°N, 16.7344136°E), in Brno City (the Red Hill section, located 49.1759981°N, 16.5864161°E), and in Prague City (the Blanka Tunnel section, 50.0974392°N, 14.4040308°E); the geographical positions of the sections are shown in Fig. 3.

The Bulhary section is located in the Dyje River Valley, which belongs to the Southern Moravian Lowland domain. The section is exposed in an abandoned loess quarry 1.2 km NW of Bulhary village. Although the section reveals erosional hiatuses, the stratigraphic settings are similar as in the Dolní Věstonice key section located 11 km NW (*Fuchs et al., 2012*). The Eemian Interglacial brown soil was developed on a top of Saalian loess. The interglacial soil is covered with early glacial chernozem overlain by last glacial loess. The erosional events were most probably triggered by slope processes.

The Red Hill section, the loess/palaeosol sequence is exposed at western edge of the town of Brno in a large abandoned loess quarry. Loess deposits including 12 pedocomplexes cover last million years (e.g., *Kukla, 1975*). The stratigraphic position of the studied section, showing loess intercalated with two palaeosol horizons, is located just above the Brunhes/Matuyama palaeomagnetic boundary.

In the Blanka Tunnel section, the loess/palaeosol sequence covers the Middle Pleistocene terrace deposited on a West bank of the Vltava River in Prague City (*Záruba et al., 1977*). The sequence was exposed during a road tunnel construction. Stratigraphic settings were estimated based on geomorphological position and relationship to the underlying river terrace. The Saalian loess is overlain by Eemian Interglacial brown soil horizon and last glacial loess. The youngest part of the section indicates sediment reworking due to slope processes. Loess is partly laminated and contains abundant clasts of local Cretaceous fine calcareous sandstone.

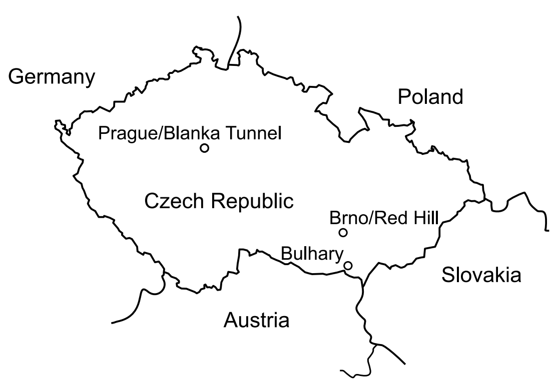

Fig. 3. Geographical positions of the loess/palaeosol sections investigated.

5. RESULTS

Figure 4a shows a plot of percentage loss of susceptibility, K_{FD}, vs. bulk susceptibility and Fig. 4b shows a plot of phase angle, δ, vs. bulk susceptibility at all three sections. Both the plots are similar. This is logical, because the K_{FD} and δ are controlled by similar fractions of magnetic minerals (see Fig. 1b), i.e. those that are magnetically viscous at the operating frequency used. The figures also show that the K_{FD} and δ increase with the susceptibility. This increase can be traditionally (since *Dearing et al., 1996*) interpreted as resulting from creation of new SP particles in soil layers during pedogenesis. Macroscopic inspection shows that the specimens with the in-phase mean susceptibility ipK_m of about 200×10^{-6} are more or less pure loess, while those with values above 400×10^{-6} are soils. This observation supports the above interpretation.

The correlation between the mean out-of-phase susceptibility and the mean parameter κ_{diff} (Eq. (5)) characterizing the frequency-dependent susceptibility is linear and excellent in all three profiles (Fig. 5). The determination coefficient, R^2, is really high, the slope of the fit straight line is very near 1, and the intercept is low. All this means that the empirical data follow the $\pi/2$ law very closely.

5.1. Red Hill in Brno

Figure 6a shows a plot of the degree of AMS vs. bulk susceptibility indicating that the *ipP*, *fdP*, and *opP* parameters continuously decrease with increasing bulk susceptibility. The lowest values are in the *ipP* parameter, while the *opP* and *fdP* values are clearly higher and mutually comparable in the majority of specimens. This can be explained by an order-of-magnitude higher grain AMS in SP particles than in MD particles.

In the shape parameter, the *ipT*, *opT* and *fdT* values may be either similar or differ moderately, but they do not differ systematically (Fig. 6b). In rough terms, one may say that the ellipsoid shapes are similar in all three anisotropy types.

In ipAMS, the magnetic foliation is roughly horizontal in average, with its poles mostly occurring in the centre of the projection net, but showing moderate plunges in

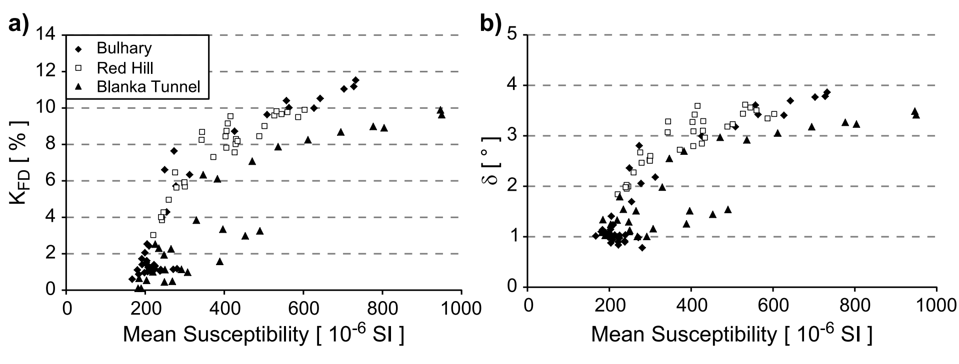

Fig. 4. a) Percentage loss of susceptibility K_{FD} and **b)** phase angle δ vs. mean susceptibility at 1220 Hz for the three studied locations.

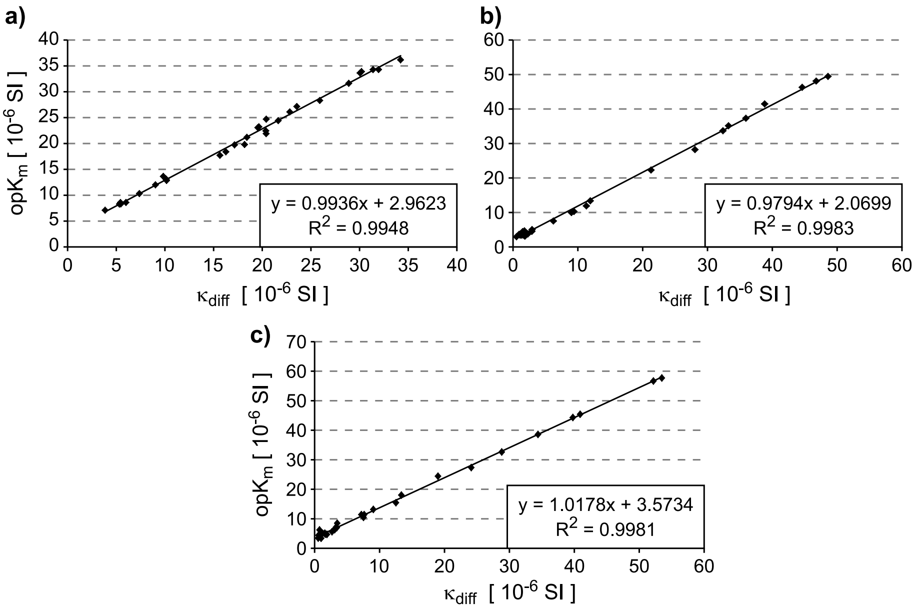

Fig. 5. Correlation between the out-of-phase susceptibility opK_m and susceptibility difference κ_{diff} at **a)** Red Hill, **b)** Bulhary, and **c)** Blanka Tunnel.

minor specimens (Fig. 6c). The magnetic lineation is sub-horizontal, creating two maxima, the major one oriented W-E and the minor one oriented N-S (Fig. 6c). The confidence areas around all three principal directions are relatively small (Fig. 6c). In fdAMS, the magnetic foliation poles create a wide and anisometric formation oriented N-S and the magnetic lineations show similar formations as in the previous case, but more scattered; the confidence areas around all three principal directions are also relatively small (Fig. 6d). In opAMS, the magnetic foliation poles tend to create an anisometric formation oriented NW-SE and the magnetic lineations show similar formations as in the previous cases, but even more scattered; the scattering is so intensive that the confidence areas around the maximum and intermediate susceptibilities partially overlap (Fig. 6e).

5.2. Bulhary

Figure 7a shows a plot of the degree of AMS vs. bulk susceptibility. The *ipP* and *opP* values are plotted for all specimens, while the *fdP* values are plotted only for specimens with *fdP* < 1.1. All the *fdP* values are shown in the inset of Fig. 7a, where they are plotted against the K_{FV} parameter, i.e. the difference between the mean susceptibility measured at 976 Hz and that measured at 156161 Hz. In specimens with $ipK_m > 400 \times 10^{-6}$, the *fdP* and *opP* values are very similar, while the *ipP* values are slightly lower (Fig. 7a). The explanation of this phenomenon may lie in an order-of-magnitude higher grain AMS in SP particles indicated by both opAMS and fdAMS than in MD particles and in a possible effect of paramagnetic minerals on the ipAMS.

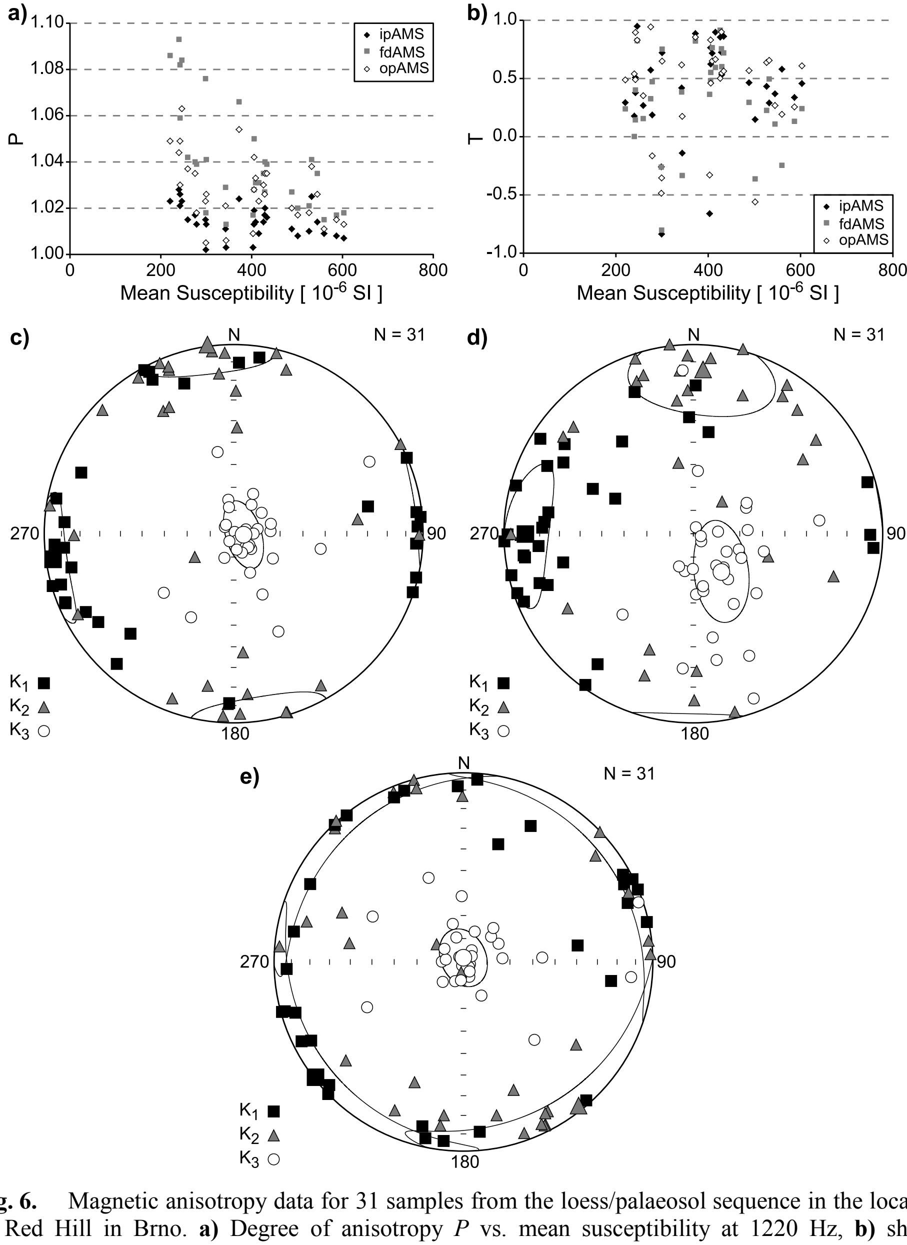

Fig. 6. Magnetic anisotropy data for 31 samples from the loess/palaeosol sequence in the locality of Red Hill in Brno. **a)** Degree of anisotropy *P* vs. mean susceptibility at 1220 Hz, **b)** shape parameter *T* vs. mean susceptibility at 1220 Hz, **c)** orientations of magnetic lineations and magnetic foliation poles for the anisotropy of in-phase magnetic susceptibility, **d)** the same as in c), but for the anisotropy of frequency-dependent susceptibility, and **e)** the same as in c), but for the anisotropy of out-of-phase magnetic susceptibility. The directional data are presented in equal-area projection on lower hemisphere. K_1, K_2 and K_3 stand for the maximum, intermediate and minimum susceptibility direction, respectively.

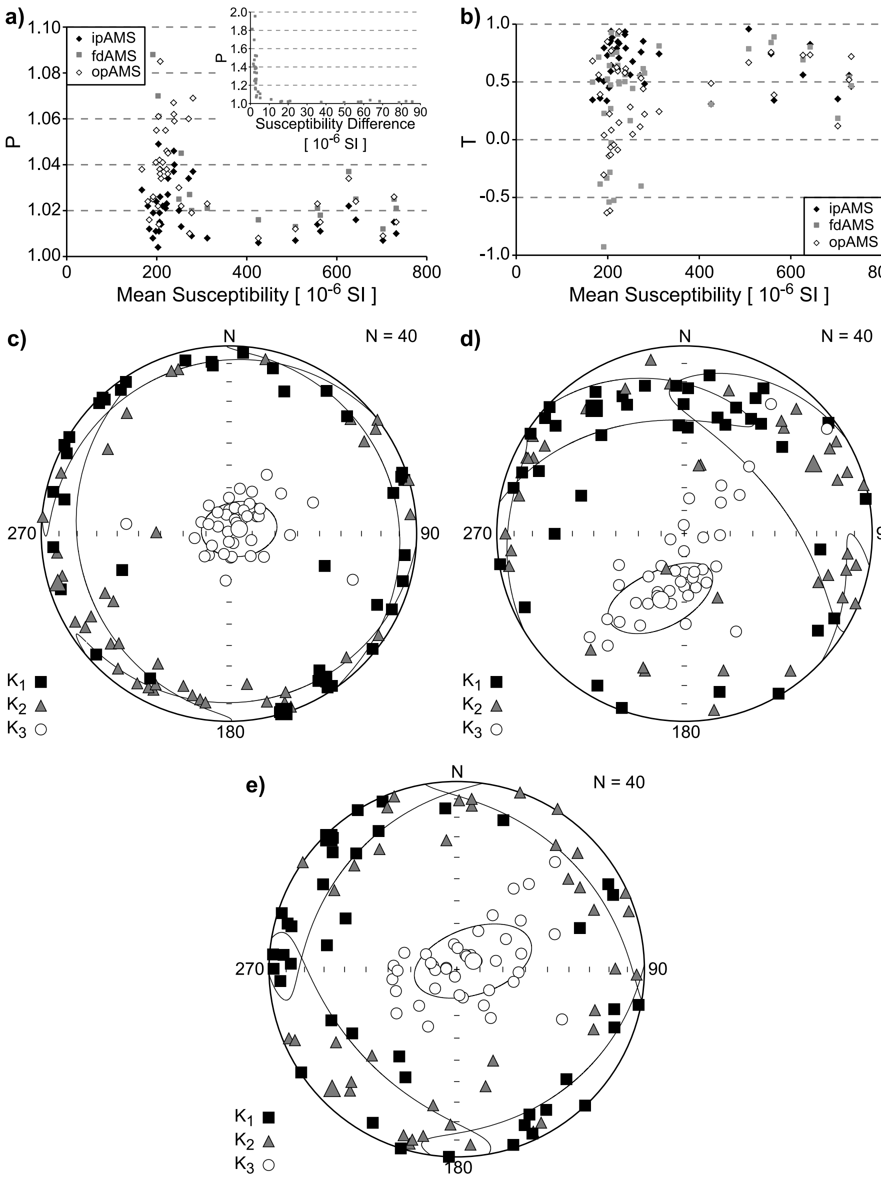

Fig. 7. The same as in Fig. 6, but for the samples from the Bulhary site.

In specimens with $ipK_m < 300 \times 10^{-6}$, all three degrees of AMS vary relatively widely (Fig. 7a). In addition, the *fdP* parameter varies extremely widely, reaching $fdP \approx 2$ in weak specimens with susceptibility difference less than 5×10^{-6} (Fig. 7a inset). Then, the extremely high *fdP* values do not likely reflect intense preferred orientation of magnetic particles, but result from insufficiently precisely determined difference susceptibilities (for details see *Hrouda, 1986, 2004*; *Hrouda and Pokorný, 2012*).

The values of the *ipT*, *opT* and *fdT* parameters may be either similar or differ moderately, but they do not differ systematically (Fig. 7b).

In ipAMS, the magnetic foliation is roughly horizontal, with its poles creating roughly concentric formation in the centre of the projection net, and the magnetic lineation is also sub-horizontal, widely scattered azimuthally (Fig. 7c). In fdAMS, the magnetic foliation poles mostly create an irregular girdle oriented NE-SW with the mean magnetic foliation dipping NE moderately (Fig. 7d). The magnetic lineations are widely scattered near the plane gently dipping NE (Fig. 7d). In opAMS, the magnetic foliation poles also create an irregular, but less pronounced, girdle oriented NE-SW and the magnetic lineations are widely scattered in the horizontal plane (Fig. 7e).

The confidence areas around the maximum susceptibility directions of all three anisotropy types (ipAMS, fdAMS, opAMS) partially overlap with the confidence areas around the intermediate susceptibility directions. This means that the magnetic lineation is not defined on the locality scale.

5.3. Blanka Tunnel in Prague

Figure 8a shows a plot of the degree of AMS vs. bulk susceptibility indicating that the *ipP*, *fdP*, and *opP* parameters continuously decrease with increasing bulk susceptibility. This decrease is very conspicuous in *fdP* and *opP* and less conspicuous, though still existing, in *ipP*. This can be again explained by an order-of-magnitude higher grain AMS in SP particles than in MD particles and by a possible effect of paramagnetic minerals on the ipAMS. The values of the *ipT*, *opT* and *fdT* parameters do not differ systematically (Fig. 8b).

In ipAMS, the magnetic foliation poles create a wide girdle oriented NW-SE (Fig. 8c). Nevertheless, the mean magnetic foliation is nearly horizontal. The magnetic lineations create a very wide sub-horizontal cluster oriented NE-SW, i.e. perpendicular to the girdle in the magnetic foliation poles (Fig. 8c). Exceptionally, the magnetic lineations are also sub-vertical. In fdAMS, the magnetic foliation poles create similar girdle oriented NE-SW, but this girdle is much narrower and dips moderately W. The magnetic lineations create a pronounced maximum oriented ENE-WSW and gently dipping WNW (Fig. 8d). In opAMS, the magnetic foliation poles create a girdle similar to that of ipAMS, i.e. oriented NW-SE, and the magnetic lineations create a well-defined sub-horizontal cluster oriented NE-SW (Fig. 8e).

6. METHODOLOGICAL IMPLICATIONS

The AMS, or better said its in-phase component, is widely used in the investigation of the preferred orientation of magnetic minerals in rocks including eolian sediments. The ipAMS is controlled by the preferred orientation of all minerals present in the rock. As the individual magnetic minerals or their fractions may show different sensitivities to various geological processes, it is desirable to investigate the magnetic sub-fabrics of individual minerals or their fractions. They can be partially investigated through the fdAMS (see *Hrouda and Ježek, 2014*) and opAMS (see *Hrouda et al., 2017*), which are solely

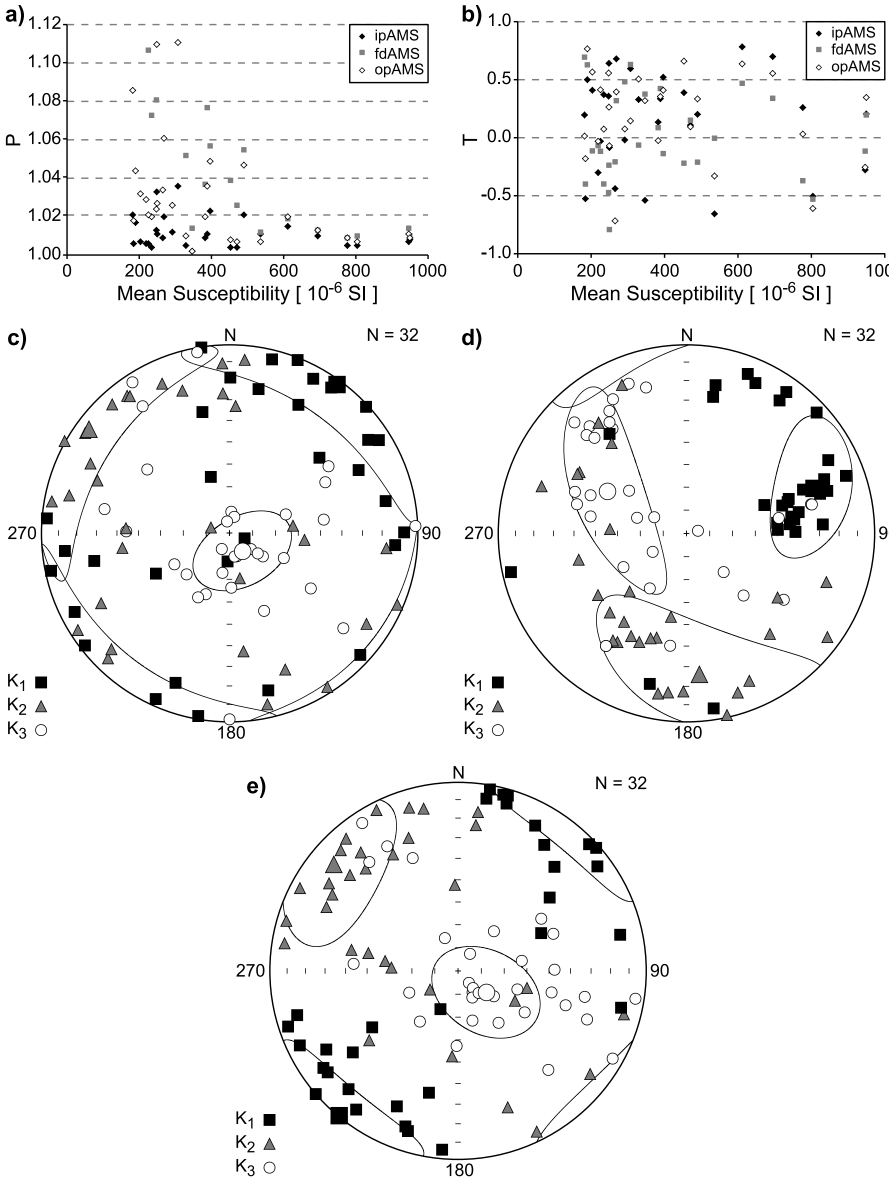

Fig. 8. The same as in Fig. 6, but for the samples from the Blanka Tunnel site.

controlled by the viscous ferromagnetic particles whereas the in-phase susceptibility of paramagnetic and diamagnetic minerals as well as of SD, MD and ultrafine purely SP ferromagnetic minerals is frequency independent and their out-of-phase susceptibility is effectively zero. It should be noted that the grain size interval of viscous particles is relatively narrow at technically feasible frequencies (see Fig. 1).

The fdAMS is determined from two independent ipAMS measurements at two frequencies. Even though each of the two measurements is very precise profiting from outstanding accuracy in measuring relative susceptibility values, the error in determination of the fdAMS is much higher, being roughly doubled (cf. *Hrouda and Pokorný, 2012*). This is because of relatively high error in the absolute susceptibility determination (due to calibration error) being about 3%. In specimens with very low susceptibility difference between low and high frequencies, typically less than 5×10^{-6}, this may result in very variable *fdP* values, which have nothing to do with extremely high variability of the preferred orientation of magnetic particles, but result from insufficient precision in the determination of susceptibility differences (for details see *Hrouda, 1986, 2004*; *Hrouda and Pokorný, 2012*).

The opAMS is measured simultaneously with the ipAMS during one measuring process so that the problem of absolute susceptibility calibration plays no role. However, there is another problem that prevents us to consider the opAMS to be superior technique. Namely, the opAMS is not measured directly, but what is measured is the overall complex susceptibility, which is subsequently resolved into the in-phase and out-of-phase components. As the out-of-phase susceptibility is usually at least an order-of-magnitude lower than the in-phase one, the error in determination of the in-phase susceptibility is similar to that of complex susceptibility, while the error in determination of the out-of-phase susceptibility may be considerably higher, mainly in specimens with very low phase angle (for details see *Hrouda et al., 2017*).

For all the reasons presented above, it is highly recommended to inspect the results of the statistical tests evaluating the precision in the determination of fdAMS or opAMS of each specimen provided by the SAFYR program and to exclude the specimens whose fdAMS and/or opAMS is determined with insufficient precision from further processing. For example, the statistical F-test, which is included in the SAFYR program, was applied to find out whether the differences between the principal susceptibilities are large enough compared to measuring errors for the specimen to be regarded as anisotropic. It showed that all the specimens investigated in the present paper are anisotropic.

In the locality of Red Hill, the percentage loss of susceptibility continuously ranges from 2% to 10% and the phase angle ranges from 2° to 4° (Fig. 4a). This indicates relatively continuous changes in the content of magnetically viscous particles. In the locality of Bulhary, there are two groups of specimens, one showing very low $K_{FD} \approx 1\%$ and $\delta = 1°$ and the other showing relatively high values $K_{FD} \approx 11\%$ and $\delta = 3.5°$. In the locality of Blanka Tunnel, the K_{FD} ranges from 1% to 10% and δ ranges from 1° to 3.5°. However, the changes are only partially continuous in two last localities, showing groups of specimens with low and high values. This may indicate layers containing magnetically viscous minerals in very low amounts and layers containing them in significant amounts.

The degrees of ipAMS, fdAMS, and opAMS decrease with increasing mean bulk susceptibility (Figs 6a, 7a, 8a), being significantly lower in soil than in loess horizons. This is in agreement with the observation by *Hus (2003)* and *Matasova and Kazansky (2004)* that in loess/palaeosol sequences the degree of AMS is lower in soil than in loess horizons, which can be explained by assuming that the preferred orientation of SP magnetic particles created during pedogenesis is much weaker than that of the other particles created during loess deposition.

The magnetic foliation poles in ipAMS are mostly vertical in the localities of Red Hill (Fig. 6c) and Bulhary (Fig. 7c) and create a wide girdle oriented NW-SE in the locality of Blanka Tunnel (Fig. 8c). In fdAMS, they create partial girdle in Red Hill (Fig. 6d) and relatively well-developed girdles in Bulhary (Fig. 7d) and in Blanka Tunnel (Fig. 8d). This may indicate that the MD particles as well as the paramagnetic particles are with their larger surfaces oriented parallel to the bedding and it was dominantly gravity that controlled this orientation. On the other hand, the viscous magnetic particles may have slightly rotated in an oriented way during their deposition or during post-depositional history.

The magnetic lineations in ipAMS, fdAMS, and opAMS are mostly sub-horizontal in all three localities. In the locality of Red Hill, the magnetic lineations show clearly bimodal distribution in ipAMS and opAMS (Fig. 6c,e) and less clearly in fdAMS (Fig. 6d). In the locality of Bulhary, the magnetic lineations show very wide (almost isotropic) azimuthal scatter in ipAMS and large almost one mode clusters in fdAMS and ipAMS with the main maxima being approximately perpendicular to the girdle in magnetic foliation poles (Fig. 7c–e). In the locality of Blanka Tunnel, the magnetic lineations create large clusters approximately perpendicular to the girdle in magnetic foliation poles in all ipAMS, dfAMS, and opAMS (Fig. 8c–e).

The magnetic lineations in wind-blown sediments, which have not been re-deposited or deformed ductilely, are parallel to the wind (e.g., *Liu et al., 1988, 2008*; *Lagroix and Banerjee, 2002, 2004b*; *Hus, 2003*; *Matasova and Kazansky, 2004*; *Zhu et al., 2000*; *Bradák, 2009*; *Bradák et al., 2011*; *Bradák and Kovácz, 2014*). This is also confirmed by deposition experiments (*Hamilton et al., 1967*; *Ellwood and Howard, 1981*). This interpretation is justified provided that the magnetic foliation is more or less horizontal. However, the magnetic foliation poles, mainly in fdAMS and opAMS, create girdle indicating at least partial fan-like orientation of magnetically viscous particles. For revealing the mechanisms of this orientation, additional sedimentological and neo-tectonic investigations are required.

7. CONCLUSIONS

The relationship between the anisotropies of frequency-dependent susceptibility (fdAMS) and out-of-phase susceptibility (opAMS) was investigated theoretically and also empirically at three loess/palaoesol profiles in Southern Moravia and in Prague. The investigation has drawn the following conclusions.

1. The fdAMS and opAMS are controlled by the magnetic particles of similar sizes. Consequently, they can serve as indicators of the preferred orientation of ultrafine magnetic particles that are on the transition between the SP and SSD states.
2. In all three profiles investigated, the correlation between the mean frequency-dependent susceptibility and mean out-of-phase susceptibility is extremely close, with the slope of the fit straight line being very near 1 and the intercept being low. All this means that the empirical data follows the $\pi/2$ law very closely.
3. The degrees of fdAMS and opAMS are higher than the degree of ipAMS evidently due to order-of-magnitude higher grain degrees of fdAMS and opAMS of

magnetically viscous particles. The degrees of fdAMS and opAMS are comparable, even though their correlation is not as excellent as that of mean susceptibilities.

4. In the loess/paleosol sequences investigated, the fdAMS and opAMS can be both coaxial with ipAMS or non-coaxial indicating slightly different orientations of viscous magnetic particles.
5. As the opAMS and fdAMS data are similar and the opAMS is measured automatically during measurement of standard AMS (ipAMS) by KLY5-A Kappabridge, the opAMS has potential to be used more frequently than the fdAMS.

Acknowledgements: The reviewers of the paper, Drs France Lagroix and Balasz Bradák, are thanked for their very constructive reviews that helped us to improve the manuscript substantially. This work was supported by the Grant Agency of the Czech Republic (research project 15-18154S [F.H, J.J.]), and Grant Agency of ASCR (research project IAAX00130801 [M.Ch.]).

References

Antoine P., Goval E., Jamet G., Coutard S., Moine O., Herisson D., Auguste P., Guerin G., Lagroix F., Schmidt E., Robert V., Debenham N., Meszner S. and Bahain J.-J., 2014. Les sequences loessiques pleistocene superieur d'Havrincourt (Pas-de-Calais, France): stratigraphie, paleoenvironnements, geochronologie et occupations paleolithiques. *Quaternaire*, **25(4)**, 321–368 (in French).

Bradák B., 2009. Application of anisotropy of magnetic susceptibility (AMS) for the determination of paleo-wind directions and paleo-environment during the accumulation period of Bag Tephra, Hungary. *Quat. Int.*, **189**, 77–84.

Bradák B. and Kovacz J., 2014. Quaternary surface processes indicated by the magnetic fabric of undisturbed, reworked and fine-layered loess in Hungary. *Quat. Int.*, **319**, 76–87.

Bradák B., Thamo-Bozso E., Kovacz J., Marton E., Csillag G. and Horvath E., 2011. Characteristics of Pleistocene climate cycles identified in Cerna Valley loess-paleosol section (Vertesca, Hungary). *Quat. Int.*, **234**, 86–97.

Chadima M. and Jelínek V., 2008. Anisoft 4.2 - Anisotropy data browser. *Contrib. Geophys. Geod.*, **38** (Special Issue), 41.

Dearing J.A., Dann R.J.L., Hay K., Lees J.A., Loveland P.J., Maher B.A. and O'Grady K., 1996. Frequency-dependent susceptibility measurements of environmental materials. *Geophys. J. Int.*, **124**, 228–240.

Egli R., 2009. Magnetic susceptibility measurements as a function of temperature and frequency I: inversion theory. *Geophys. J. Int.*, **177**, 395–420.

Ellwood B.B. and Howard J.H., 1981. Magnetic fabric development in an experimentally produced barchan dune. *J. Sedim. Petrol.*, **51**, 97–100.

Fuchs M., Kreutzer S., Rousseau D.D., Antoine P., Hatté Ch., Lagroix F., Moine O., Gauthier C., Svoboda J. and Lisá L., 2012. The loess sequence of Dolní Věstonice, Czech Republic: A new OSL-based chronology of the Last Climatic Cycle. *Boreas*, **42**, 664–677.

Hamilton N., Owens W.H. and Rees A.I., 1968. Laboratory experiments on the production of grain orientation in shearing sand. *J. Geol*., **76**, 465–472.

Heller F. and Evans M.E., 2003. *Environmental Magnetism: Principles and Applications of Anviromagnetics*. Academic Press, New York.

Hrouda F., 2011. Models of frequency-dependent susceptibility of rocks and soils revisited and broadened. *Geophys. J. Int*., **187**, 1259–1269.

Hrouda F. and Pokorný J., 2011. Extremely high demands for measurement accuracy in precise determination of frequency-dependent magnetic susceptibility of rocks and soils. *Stud. Geophys. Geod*., **55**, 667–681.

Hrouda F. and Pokorný J., 2012. Modelling accuracy limits for frequency-dependent anisotropy of magnetic susceptibility of rocks and soils. *Stud. Geophys. Geod*., **56**, 789–802.

Hrouda F. and Ježek J., 2014. Frequency-dependent AMS of rocks: A tool for the investigation of the fabric of ultrafine magnetic particles. *Tectonophysics*, **629**, 27–38.

Hrouda F. and Ježek J., 2017. Role of single-domain magnetic particles in creation of inverse magnetic fabrics in volcanic rocks: A mathematical model study. *Stud. Geophys. Geod*., **61**, 145–161, DOI: 10.1007/s11200-015-0675-6.

Hrouda F., Pokorný J., Ježek J. and Chadima M., 2013. Out-of-phase magnetic susceptibility of rocks and soils: a rapid tool for magnetic granulometry. *Geophys. J. Int*., **194**, 170–181, DOI: 10.1093/gji/ggt097.

Hrouda F., Chadima M., Ježek J. and Pokorný J., 2017. Anisotropy of out-of-phase magnetic susceptibility of rocks as a tool for direct determination of magnetic subfabrics of some minerals: an introductory study. *Geophys. J. Int*., **208**, 385–402.

Hus J.J., 2003. The magnetic fabric of some loess/palaeosol deposits. *Phys. Chem. Earth*, **28**, 689–699.

Jackson M., 2003. Imaginary susceptibility, a primer. *IRM Quarterly*, **13(4)**, 1, 10–11.

Jelínek V., 1978. Statistical processing of magnetic susceptibility measured on groups of specimens. *Stud. Geophys. Geod*., **22**, 50–62.

Jelínek V., 1981. Characterization of magnetic fabric of rocks. *Tectonophysics*, **79**, T63–T67.

Kukla G., 1975. Loess stratigraphy of central Europe. In: Butzer K.W. and Isaac G.L. (Eds), *After the Australopithecines*. De Gruyter/Mouton Publishers, Den Haag, The Netherlands, 99–188.

Lagroix F. and Banerjee S.K., 2002. Paleowind directions from the magnetic fabric of loess profiles in central Alaska. *Earth Planet. Sci. Lett*., **195**, 99–112.

Lagroix F. and Benerjee S.K., 2004a. The regional and temporal significance of primary aeolian magnetic fabrics preserved in Alaskan loess. *Earth Planet. Sci. Lett*., **225**, 379–395.

Lagroix F. and Banerjee S.K., 2004b. Cryptic post-depositional reworking in aeolian sediments revealed by the anisotropy of magnetic susceptibility. *Earth Planet. Sci. Lett*., **224**, 453–459.

Liu X., Xu T. and Liu T., 1998. The Chinese loess in Xifeng, II: A study of anisotropy of magnetic susceptibility of loess from Xifeng. *Gophys. J*., **92**, 349–353.

Liu P., Jin C.S., Zhang S., Han J.M. and Liu T.S., 2008. Magnetic fabric of early Quaternary loess-paleosol of Longdan Profile in Gansu Province and the reconstruction of the Paleowind directions. *Chinese Sci. Bull*., **53**, 1450–1452.

Matasova G.G. and Kazansky A.Yu., 2004. Magnetic properties and magnetic fabrics of Pleistocene loess/palaeosol deposits along west-central Siberian transect and their palaeoclimatic implications. In: Martín-Hernández F., Lüneburg C.M., Aubourg C. and Jackson M. (Eds), *Magnetic Fabric:Methods and Applications*. *Geol. Soc. London Spec. Publ.*, **238**, 145–173.

Nagata T., 1961. *Rock Magnetism*. Maruzen, Tokyo, Japan.

Neél L., 1949. Théorie du trainage magnétique des ferrimagnétiques en grains fins avec applications aus terres cuites. *Ann. Géophys*., **5**, 99–136 (in French).

Pokorný J., Pokorný P., Suza P. and Hrouda F., 2011. A multi-function Kappabridge for high precision measurement of the AMS and the variations of magnetic susceptibility with field, temperature and frequency. In: Petrovský E., Herrero-Bervera E., Harinarayana T. and Ivers D. (Eds), *The Earth's Magnetic Interior*. Springer-Verlag, Heidelberg, Germany, 292–301.

Pokorný P., Pokorný J., Chadima M., Hrouda F., Studýnka J. and Vejlupek J., 2016. KLY5 Kappabridge: high sensitivity and anisotropy meter precisely decomposing in-phase and out-of-phase components. *Geophys. Res. Abstr.*, **18**, EGU2016-15806.

Shliomis M.I. and Stepanov V.I., 1993. Frequency dependence and long time relaxation of the susceptibility of the magnetic fluids. *J. Magn. Magn. Mater.*, **122**, 176–181.

Shcherbakov V.P. and Fabian K., 2005. On the determination of magnetic grainsize distributions of superparamagnetic particle ensembles using the frequency dependence of susceptibility at different temperatures. *Geophys. J. Int.*, **162**, 736–746.

Svendlidh P., Jonsson T. and Garcia-Palacios J.L., 1997. Intra-potential-well contribution to the AC susceptibility of a noninteracting nano-sized magnetic particle system. *J. Magn. Magn. Mater.*, **169**, 323–334.

Taylor S.N. and Lagroix F., 2015. Magnetic anisotropy reveals the depositional and postdepositional history of a loess-paleosol sequence at Nussloch (Germany). *J. Geophys. Res*. *Sol. Earth*, **120**, 2859–2876.

Worm H.-U., 1998. On the superparamagnetic - stable single domain transition for magnetite, and frequency dependence of susceptibility. *Geophys. J. Int.*, **133**, 201–206.

Záruba Q., Bucha V. and Ložek V., 1977. Significance of the Vltava terrace system for Quaternary chronostratigraphy. *Rozpravy ČSAV*, **87(4)**, Academia, Prague, Czech Republic.

Zhu R., Kazansky A., Matasova G., Guo B., Zykina V., Petrovsky E. and Jordanova N., 2000. Rock-magnetic investigation of Siberia loess and its implications. *Chinese Sci. Bull.*, **45**, 2192–2198.